Nuclear Instruments and Methods in Physics Research A259 (1987) 119–124
North-Holland, Amsterdam

Section III. Unconventional experiments

RECENT MEASUREMENTS OF ELECTRON TRAPPING AND PHASE AREA DISPLACEMENT OF NONRELATIVISTIC ELECTRONS EMPLOYING AN ELECTROMAGNETIC WIGGLER

R.Z. OLSHAN, S. RUSCHIN, A. GOVER, H. KLEINMAN, B. LISSAK and Z. SHEENA

Faculty of Engineering, Tel-Aviv University, 69978 Ramat-Aviv, Israel

We report the distinct observation of electron trapping and phase area displacement energy transfer mechanisms in a stimulated Compton scattering free electron laser scheme. The synchronous energy exchange occurred between nonrelativistic electrons and the ponderomotive (beat) force of two counter-propagating intense pulsed CO_2 laser beams. The direction of the energy exchange was dependent on the position where synchronism occurred in the interaction region, as predicted by theory for electron trapping and phase area displacement.

1. Introduction

In an on-going experiment at Tel-Aviv University, we have recently demonstrated energy transfer between nonrelativistic electrons and the ponderomotive potential of two counter-propagating CO_2 laser beams operating at different frequencies. We previously reported [1] the first results of the experiment wherein a synchronous energy transfer effect was detected when a nonrelativistic electron beam attained synchronism with the ponderomotive potential wave resulting from two counter-propagating CO_2 lasers. In this report we demonstrate that energy transfer was induced by both electron trapping and phase area displacement mechanisms [2,3].

The FEL efficiency enhancement scheme of a tapered-period static wiggler with a decelerating beat wave has essentially the same physics as the axial E-field scheme [2]. Such FELs were recently demonstrated to operate with remarkable efficiencies [4]. Laser accelerators with inverse tapering have been considered [5], and PAD-FEL accelerator schemes have been proposed [2,3], but neither have yet been tried. Our experiment has been designed for investigating nonlinear-regime stimulated Compton scattering in the travelling beat wave of two counter-propagating laser beams. Specifically it serves to investigate the physics of FEL efficiency enhancement mechanisms, such as electron trapping and phase area displacement (PAD), which can occur in tapered wiggler FELs or in FELs with externally applied axial electric fields.

A description of the electron trapping and PAD energy transfer mechanisms associated with both the tapered wiggler and the axial E-field enhancement schemes can be obtained with the aid of fig. 1. For a more detailed description and analysis the reader is referred to refs. [1,2]. Both mechanisms require synchronism of the electron velocity with the ponderomotive (beat) wave velocity given by

$$v_r = \frac{\omega_s - \omega_w}{k_s + k_s}. \tag{1}$$

In the case of a static wiggler $\omega_w = 0$. Electron trapping occurs when the electrons are initially synchronous with the deep ponderomotive potential wells (traps). The phase diagram of fig. 1a depicts partial initial trapping in a tapered wiggler efficiency enhancement scheme. As the electrons lose energy by radiating into the signal field, their velocity decreases and the radiative process becomes saturated. The tapering of the wiggler period induces the trapped electrons to continue to radiate past the saturation point of a constant period wiggler. The analogous trapped electron efficiency enhancement scheme with an applied axial E field is illustrated in the phase space diagram of fig. 1b. Electrons initially trapped by a constant velocity ponderomotive potential wave do not accelerate, and consequently the energy invested by the external axial field produces enhanced stimulated Compton scattering radiation into the signal field. Figs. 1c and 1d depict an alternative mechanism of radiative energy extraction called phase area displacement [2,3], which results in enhanced signal amplification when the entire e-beam is scanned through the synchronism condition at any point along the interaction length without electron trapping. In PAD, as opposed to electron trapping, signal amplification is accomplished by either reversing the taper in a tapered wiggler, or by reversing the polarity of the dc field. In both of these PAD schemes, all the electrons are scanned through the energy of synchronism and result in a net energy extraction from the entire electron beam. Note that for axial field acceleration with the same polarity dc field, the trapped electron and the PAD mechanisms

0168-9002/87/$03.50 © Elsevier Science Publishers B.V.
(North-Holland Physics Publishing Division)

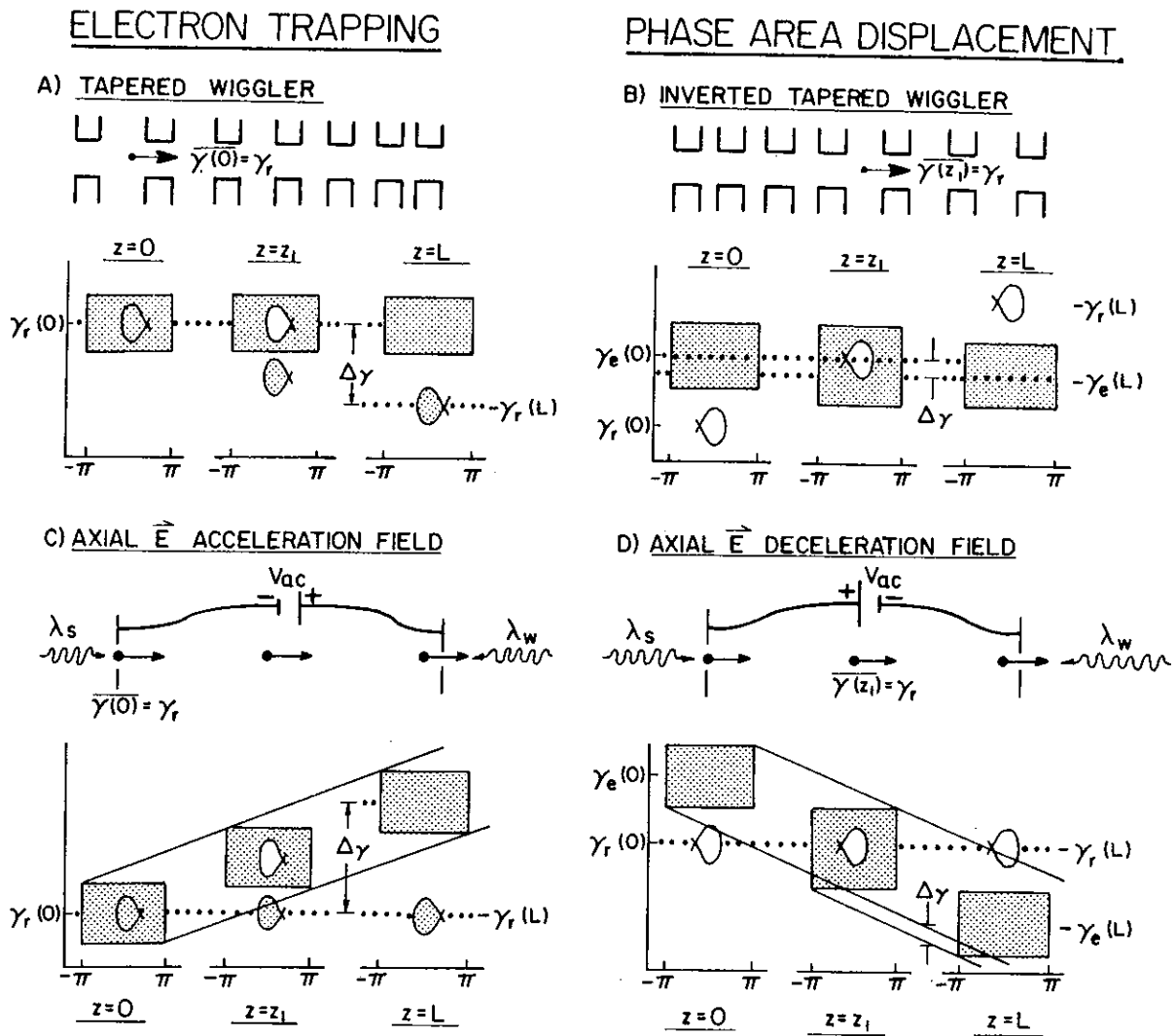

Fig. 1. Phase space diagrams for electron energy extraction: (a) Electron trapping with a tapered wiggler; (b) Phase area displacement with an inverted tapered wiggler; (c) Electron trapping with an axial acceleration field; (d) Phase area displacement with an axial deceleration field.

would result in energy exchange with the radiation fields in opposite directions.

2. The experiment scheme

The experiment concept, as depicted in fig. 2, was described in detail in ref. [1]. Two TEA CO_2 lasers produced the 9.3 μm signal wave and the 10.6 μm wiggler wave, both of which were operated in single longitudinal and transverse cavity modes. Their 100 ns duration pulses were synchronized to arrive simultaneously at the interaction region during the 10 μs pulse of the electron beam. The ~ 1 kV electron beam voltage was matched to the synchronism condition eq. (1), at either the entrance to the interaction region for setting trapping conditions (fig. 1c), or within the interaction region for PAD (fig. 1d). The e-beam energy spread was $\Delta E_{th} \approx 4$ eV, with a grid controlled current of 10–50 μA.

An axial electric force was exerted along the interaction length by employing a 1 ms, 300 A current pulse to a copper coil surrounding the e-beam as a result of the ohmic potential drop along the coil. Accelerating or decelerating fields were achieved by changing the direction of the current. The coil current also provided an axial magnetic field which bent the e-beam and guided it along the interaction region.

Time-of-flight energy analysis is performed on the electrons. After exiting the interaction region, the elec-

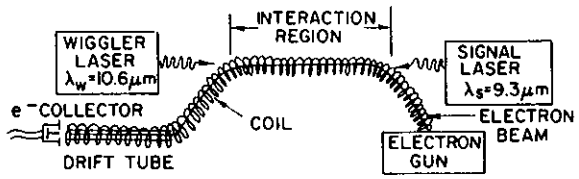

Fig. 2. Experiment schematic.

trons enter the drift tube which is biased with a low voltage ($V_{dt} = 10$ V), so that electrons of different velocities, and corresponding different drift times, produce a time-dispersed current pulse which folds in it the electron energy spectrum after the interaction.

The electron current pulse and the laser pulses were recorded by three separate channels of high-speed digital transient recorders. The data was stored by an on-line computer for subsequent reduction, analysis and interpretation.

3. Theory

The basic theory of electron trapping and PAD efficiency enhancement schemes in magnetic bremsstrahlung FELs is given in refs. [2,3]. The electron axial motion is governed by the longitudinal force equation

$$\frac{\mathrm{d}(\gamma m v_z)}{\mathrm{d}t} = -eE_{ac} - eE_p \cos\psi(z, t), \tag{2}$$

where E_{ac} is an externally applied axial accelerating or decelerating dc electric field, and E_p is the ponderomotive field amplitude, which for the case of an e.m. wiggler is given by [6]

$$E_p = \frac{e(\mu_0/\epsilon_0)^{1/2}}{\gamma_r mc^2}(\lambda_s + \lambda_w)\,|\hat{e}_s \cdot \hat{e}_w^*|\,\frac{(P_w P_s)^{1/2}}{\pi w_{0s} w_{0w}}, \tag{3}$$

where $\hat{e}_i$, P_i, w_{0i} $(i = \mathrm{w}, \mathrm{s})$ are the polarization unit vectors, the powers and beam waists of the wiggler and signal waves respectively. The phase of the electron relative to the ponderomotive wave is

$$\psi = (\omega_s - \omega_w)t - (k_s + k_s)z.$$

First integration of the pendulum-like equation (2) results in closed (trapped) or open electron phase-space orbits inside or outside the separatrix respectively. The separatrix function (shown in fig. 1) is characterized by two parameters: the resonant phase ψ_r; and the zero field half width (HW) of the trap $\delta\gamma_t^0$ given by [5]

$$\psi_r = \arcsin\left(\frac{E_{ac}}{E_p}\right), \tag{4}$$

$$\delta\gamma_t^0 = \left(\frac{4e\beta^2\gamma^3 E_p}{(k_s + k_s)mc^2}\right)^{1/2}. \tag{5}$$

For $\psi_r = 0$, the separatrix function is simply $\delta\gamma = \delta\gamma_t^0\,|\cos(\psi/2)|$. For $\psi_r \neq 0$, it is given by another periodic function with reduced phase-space dimensions of the trap [2,3]: $\delta\gamma_m < \delta\gamma_t^0$, $\Delta\psi < 2\pi$. With uniform acceleration along the interaction region, electrons that are trapped inside the interaction region remain trapped to the end (fig. 1c), and are displaced by an average energy $\Delta\bar{\gamma}$, relative to the untrapped ones, where

$$\delta\bar{\gamma}_{trap} = \frac{eE_{ac}L}{mc^2}, \tag{6}$$

and L is the interaction length. For a warm electron beam, $\Delta\gamma_{th} \gg 2\delta\gamma_m$, the trapping efficiency will be at most $A_t/(2\pi\Delta\gamma_{th})$, where A_t is the trap area ($A_t \approx 8\delta\gamma_t^0$ for $\psi_r \ll 1$).

If the decelerated or accelerated e⁻ beam synchronizes with the beat wave within (as opposed to at the start of) the interaction region (fig. 1d), the beam will exchange average energy $\Delta\bar{\gamma}_{PAD}$ with the radiation field by the PAD mechanism. $\Delta\bar{\gamma}_{PAD}$ may be calculated by integration along phase-space paths of the electrons. For $\psi_r \ll 1$, neglecting edge effects, an approximate expression is derived [2,3]:

$$\Delta\bar{\gamma}_{PAD} \cong A_t/2\pi = 4\delta\gamma_t^0/\pi. \tag{7}$$

This average energy transfer will affect all the electrons, even if the initial e-beam energy spread is large, since they all pass through synchronism with the beat wave.

4. Experimental results

The experiment previously reported [1] employed a retarding potential method for electron energy analysis. In that experiment the initial energy of the beam was scanned to vary the position of synchronism along the interaction region and a decelerating axial field was used. The signal intensity, which is proportional to the number of electrons acquiring energy from the radiation

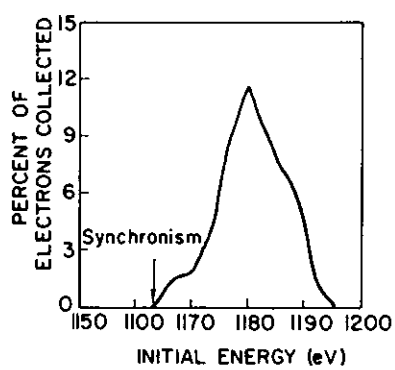

Fig. 3. Collector current signal vs initial electron energy. The arrow marks synchronism at the entrance to the interaction region.

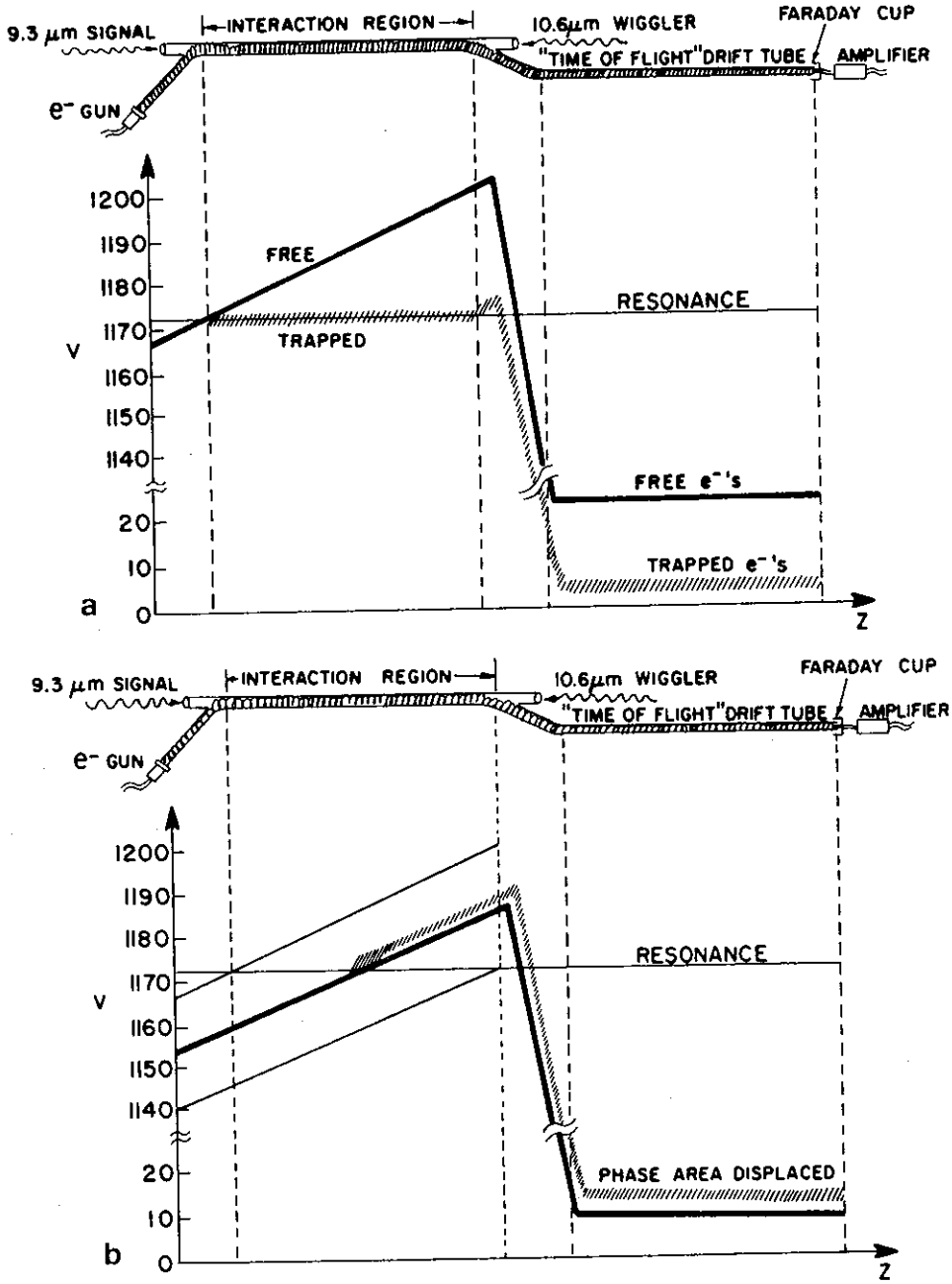

Fig. 4. Kinetic energy variations along the experiment system for: (a) Electron trapping, $V_i = 1166$ V; (b) Phase area displacement, $V_i = 1155$ V.

field, exhibited a resonance curve as a function of V_i as shown in fig. 3. The peak of the curve corresponds to beam energy at synchronism condition with the beat wave in the center of the interaction region, where the laser fields were most intense. Its width corresponds to the potential drop along the interaction region ($E_{ac}L = 40$ V). These findings correspond well with a PAD interaction interpretation.

The retarding potential method does not give the electron energy spectrum in a single pulse; moreover, the energy exchange in the interaction turned out to be smaller than the initial energy spread. It was hard, therefore, to resolve the direction of net energy transfer between the beam and the radiation field with the retarding potential technique. In order to resolve this problem and distinctly identify the occurrence and con-

Table 1
Experiment parameters

Signal power	0.25 MW
Wiggler power	0.25 MW
Signal wavelength	9.261 μm
Wiggler wavelength	10.59 μm
Optical beam waists diameter	2 mm
Coil current	0.3 kA
Energy spread (fwhm)	3 eV
Interaction length	0.6 m
Electron current	10 μA
Electron velocity	2.0×10^7 m/s
Axial electric field	42 V/m
Resonance energy	1.153 keV
Ponderomotive field	369.7 V/m
Trap depth	1.409 eV
Resonant phase ψ_r	0.2 rad

ditions for trapped electron and PAD interaction effects, we revised the experimental set-up to include a time of flight energy analysis tube.

The kinetic energy of the electrons is followed through the system in fig. 4 for an accelerating axial field configuration, and illustrates the energy transfer expected for electron trapping and PAD. The axial electric field uniformly accelerates the free electrons through the interaction region, at which they are decelerated and drift at a low potential though the time of flight tube, as illustrated in fig. 4a. For an initial potential of 1165 V, the electrons become resonant with the ponderomotive potential at the start of the interaction region. As illustrated, the trapped electrons remain synchronous with the ponderomotive wave and do not experience the acceleration in the interaction region. The trapped electrons thus propagate through the drift tube with less energy and arrive later at the collector. This would result in a deficiency in the collected electron signal after the lasers pulse, followed by an excess current signal when the trapped electrons arrive.

By simply reducing the initial potential by some small incremental amount (2–3 eV), PAD occurs instead of electron trapping, hence the direction of energy transfer is reversed as illustrated in fig. 4b. The electrons become synchronous with the ponderomotive wave somewhere in the middle of the interaction region, at which point all of the electrons experience additional acceleration due to the ponderomotive force. This results in a net average acceleration to the electron beam during the pulse of the lasers. The collector would then detect an excess electron current pulse followed by a current deficient pulse, which is opposite of that expected for the electron trapping mechanism.

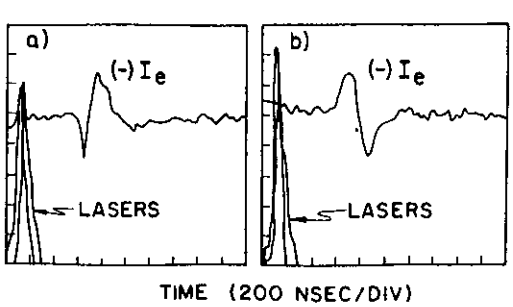

Fig. 5. Collector current signals corresponding to electrons (a) accelerated and (b) decelerated by the radiation field.

The experiment was operated with the parameters given in Table 1. The experimental results are shown in fig. 4. The oscillograms display the measured collector current signal for two values of initial voltage of the beam: $V_i = 1155$ V corresponding to synchronism near the center of the interaction region (fig. 5a), and $V_i = 1165$ V corresponding to synchronism right at the entrance to the interaction region (fig. 5b). In both cases the signals appear with a transit time delay (~ 0.6 μs) relative to the concident laser pulses, but the signals are temporally inverted relative to each other, indicating opposing energy transfer directions. The oscillogram of fig. 5a with an initially negative (excess current) signal followed by a positive (charge depletion) signal, indicates net electron acceleration by the laser pulses, and corresponds to the expectations for PAD energy exchange. Conversely, the signal of fig. 5b indicates electron deceleration and thus energy transfer to the radiation field in agreement with predictions for electron trapping.

5. Conclusion

The experimental data demonstrates that both trapping and PAD mechanisms of energy exchange were observed in the stimulated Compton scattering scheme at the conditions predicted by theory. Due to the large initial beam energy spread, which was apparently as large as the net energy transfer, the signals were not completely resolved in time, and it was hard to determine the exact amount of energy exchanged with the radiation field in either mechanism. However, simulation of the drift tube transport dynamics with the known initial electron energy distribution (measured by scanning the retarding potential) and with assumptions of energy transfer $\Delta\bar{E} \approx +1.5$ eV and $\Delta\bar{E} \approx -2.0$ eV fitted reasonably well with the waveforms of figs. 5a and 5b respectively. The +1.5 eV PAD energy transfer compares well with the $\bar{E} \approx 1.6$ eV predicted from eq. (7). The −2.0 eV energy transfer corresponds to electron detrapping after 5 cm, possibly due to nonuniformities in the dc fields, lateral deviations in the overlapping of the beams, or the finite coherence of the laser beams.

The successful demonstration of energy exchange by nonlinear regime Compton scattering in the present

experiment, makes way for further fundamental interaction and FEL related studies in a small scale laboratory system. Continuation of this experiment will provide opportunities to further study important interaction aspects of phase area displacement and trapping mechanism; for example, effects of non-adiabatic changes in the interaction parameters and incoherence of the wiggler and signal waves. The large number of wiggler periods (5×10^4) and trap synchrotron oscillations (~ 40) puts this lasers' beat experiment in the interesting regime of very long wiggler FELs and laser accelerators, where studies of phase space evolution has important fundamental and applied research implications.

Acknowledgement

This work was supported initially by USAF grant AFOSR 82-0239 and subsequently by endowments from the Kranzberg Inst. and Israeli Universities funding committee. A. Friedman, B. Cohen and P. Yogev made important contributions to the experiment construction. We thank C. Brau and P. Morton for suggesting the PAD scheme as an interpretation to our early experimental results.

References

[1] R.Z. Olshan, A. Gover, S. Ruschin, H. Kleinman, A. Friedman, B. Steinberg and I. Katz, Nucl. Instr. and Meth. A250 (1986) 253.
[2] N.M. Kroll, P. Morton and M.N. Rosenbluth, IEEE J. Quantum Electron. QE-17 (1981) 1436.
[3] M.N. Rosenbluth, B.N. Moore and H.V. Wong, IEEE J. Quantum Electron. QE-21 (1985) 1026.
[4] C.A. Brau, IEEE J. Quantum Electron. QE-21 (1985) 824; T.J. Orzechowski et al., ibid., p. 831.
[5] E.D. Courant, C. Pellegrini and W. Zakowicz, Phys. Rev. A32 (1985) 2813.
[6] R.Z. Olshan, Ph.D. Dissertation, Tel-Aviv University (1986).